

The Use of Mathematical Finite Element Method to find the Optimum Waves Amplification by a Novel Elliptical Waveguide

*Zeinab Rahmani**

Abstract

In this paper, a combinatorial elliptic-circular waveguide is introduced to amplify electromagnetic waves. The cross-section of this waveguide is elliptic and filled by a dielectric medium; while two axial circular cavities have been created in it, just outside the center. A cavity has been filled by an unmagnetized cold plasma and a relativistic pencil electron beam (RPEB) is injected in other cavity. By applying an adaptive finite element method (FEM), electromagnetic slow waves amplification in the waveguide is investigated. We study variations of growth rate of excited microwaves under influence of different factors. The purpose of examining the effect of various parameters of this waveguide such as plasma and electron beam radiuses, the RPEB location, dielectric constant and beam current intensity; is to introduce the waveguide with optimal configuration and parameters to obtain the highest wave growth rate.

Keywords: combinatorial dielectric-plasma waveguide, relativistic pencil electron beam, time growth rate, finite element method.

2010 Mathematics Subject Classification: 65N25, 78M10.

How to cite this article

Z. Rahmani, On the optimal design of an elliptical dielectric waveguide including axial circular hollows filled by plasma and electron beam for waves amplification, *Math. Interdisc. Res.* 1 (202x) xx-yy.

1. Introduction

Waveguides are structures that are used for guiding waves as electromagnetic and sound waves and applied in order to effective transmission of electromagnetic power

*Corresponding author (E-mail: z.rahmani@kashanu.ac.ir)

Academic Editor: Majid Monemzadeh

Received 24 July 2020, Accepted 21 June 2021

DOI: 10.22052/MIR.2021.240214.1229

from one point to another in space [11]. Waveguides with different structures and materials, are proposed and applied for various aims [12],[10]. Actually, the structure selection depends on the operating frequency band, the amount of transmitting power and the transmission losses [12]. Although, a large number of empirical and theoretic researches have been done on waveguides with rectangular, triangle, circular and elliptic cross-sections [2,7]; but so far few scientific articles have been published about waveguides with combined geometries. In 1997, Benito Gimeno et al. applied an efficient method to achieve the modal spectrum of elliptic waveguides and investigation of the connections between squar, circular, or elliptic to elliptic waveguides [4]. Then, the electromagnetic wave scattering from an elliptic dielectric column, covering peculiarly a circular metallic [17], and scattering by a circular dielectric layer coating eccentrically an elliptic dielectric column, had been investigated [18,23]. At first, Shahi et al. analyzed a circularly cored highly birefringent (Hi-Bi) waveguide for the first time, in 2007 [19]. Afterwards, excitation and amplification of electromagnetic waves in a combined dielectric waveguide was investigated in 2019 [13].

Several methods as Integral Equation, Finite Element, Transverse Resonance and Point Matching methods, have been developed to solve the vector-wave equation of a waveguide with an arbitrary cross section [16,22]. The finite element method is known as a suitable approach to be applied in waveguides with complicated and inhomogeneous structure. Finite element method has been used to discuss the dominant mode in a simple elliptical waveguide and the electrical field lines of the dominant TE mode and the magnetic field lines of the lowest TM mode [8]. Field patterns in V-shaped micro-shield transmission line have been calculated by using the edge-based finite element method [9]. The possibility of plasma wave simulation based on the finite element method has been examined, and a full wave simulation code of the lower hybrid wave was developed [20].

In the current work, we will investigate an elliptical waveguide including an isotropic cold plasma column with circular cross-section that is placed in focus of the waveguide. A relativistic solid electron beam has been injected in elliptic waveguide in order to amplification of the electromagnetic waves. It should be added that the rest of the waveguide space is filled with dielectric material to decrease the phase velocity of the propagated waves and excitation of slow waves. Here the excited waves have nonzero field component along the beam velocity $\vec{E} \cdot \vec{V}_0 \neq 0$, and consequently the field can influence the beam electrons. The beam can be decelerated by the field, thus transmission part of its energy to the wave. The wave emerging from an initial fluctuation increases with time. This increment is most important in the frequency range of the Cherenkov resonance [1]. We will attain the global generalized eigenvalue equation of the system by solving the fluid and Maxwell's equations for the dielectric, beams and plasma mediums. Such a non-isotropic combinatorial plasma-dielectric waveguide, has been adjusted from elliptic laser pumping cavities [3]. Characteristic eigenvalue equation and dispersion relation of this structure will be found by applying finite element method (FEM). The newness of this work alludes to this subject, the plasma effect on the

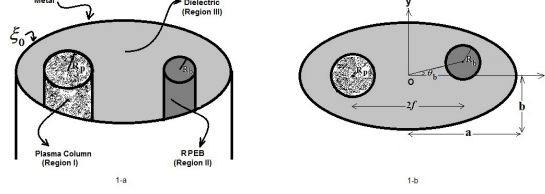


Figure 1: Geometric schematic of the elliptical waveguide with two hollows filled by a plasma column and an electron beam.

excitation and amplification of electromagnetic waves in a waveguide with such complicated configuration that has a junction between circular and elliptical geometries has been investigated. As known the elliptical waveguides have a higher growth rate for excited slow waves in comparison with circular cylindrical and slab waveguides. With attention to different variable parameters considered in the present structure such as geometric configuration including radiuses of plasma and electron beam columns and location of the beam, dielectric permittivity and current intensity of the electron beam, we can determine optimal design for obtaining maximum wave amplification. It will be seen that by using the novel waveguide introduced in this article, microwaves excitation with higher growth rate can accrue in comparison with other dielectric-plasma waveguides.

The present work has been arranged in four sections where the Introduction was presented as Section 1. The waveguide configuration and fundamental equations of problem is presented in Section 2. In Section 3, the numerical outcomes and diagrams of dispersion relations and time growth rate for excitation of slow waves will be presented. Ultimately, a summary and conclusion are presented in Section 4.

2. Configuration and Fundamental Equations

In the present study, as illustrated in Figure 1-a, an elliptical dielectric waveguide with completely conducting walls and relative permittivity ϵ_r including two axial circular hollows, is considered. One of the hollows with radius R_p that created in the left focus of the elliptical waveguide is filled by an unmagnetized cold plasma with equilibrium density N_{p0} . On the other hand, as shown in Figure 1-b, another hollow with radius R_b is situated in right focus or slightly shifted from it under angle θ_b . A relativistic pencil electron beam, (RPEB), with a uniform current density is injected in the second hollow. It must be mentioned two hollows are fully filled by plasma and RPEB, so it can be said the waveguide consists of three region plasma, electron beam and dielectric. The equilibrium velocity and density of the relativistic electron beam are defined respectively as $V = V_0 \hat{z}$ and N_{b0} , where \hat{z} is the unit vector along the symmetry axis of the electron beam column. In the

present work, we consider ions of plasma as motionless because of their heavier mass. Therefore, in the linear approximation, the perturbed current density and perturbed charge density of electrons in plasma and RPEB, can be found by the relativistic momentum transfer and continuity equations as follows [1], [5]:

$$\left[\frac{\partial}{\partial t} + \vec{V} \cdot \vec{\nabla} \right] \frac{\vec{V}}{\sqrt{1 - \frac{V^2}{c^2}}} = \frac{-e}{m_0} \left[\vec{E} + \frac{\vec{V}}{c} \times \vec{B} \right], \quad (1)$$

$$\frac{\partial N}{\partial t} + \vec{\nabla} \cdot (N \vec{V}) = 0, \quad (2)$$

where c is the light velocity in vacuum, e and m_0 are the electric charge and rest mass of electron, respectively. On the other hand, it must be noted the electron beam is assumed to be focused by a infinitely intense axial magnetic field so that the transverse motion of the electrons of beam is negligible. Under this conditions, and with linearizing Equations (1) and (2), the perturbed current and charge densities of electrons in the plasma column and RPEB can be written in terms of the fluctuation of electric field [14,15]. Then by applying the perturbed quantities obtained from fluid equations that are written as a superposition of monochromatic plane waves of the form $\delta\psi = \delta\psi_0 e^{j(k_z z - \omega t)}$, and doing some uncomplicated computing, one can obtain dielectric tensor of cold isotropic plasma and RPEB regions. In this approach, system of Maxwell's equations

$$\vec{\nabla} \times \vec{E} - j\omega \vec{B} = 0, \quad (3)$$

$$\vec{\nabla} \times \vec{B} + j\omega\mu_0 \tilde{\epsilon} \vec{E} = 0, \quad (4)$$

where $\vec{B} = \mu_0 \vec{H}$, will be used in three regions plasma(I), RPEB(II) and dielectric(III) with dielectric tensors $\tilde{\epsilon}$:

$$\tilde{\epsilon} = \epsilon_0 \begin{pmatrix} 1 - \frac{\omega_p^2}{\omega^2} & 0 & 0 \\ 0 & 1 - \frac{\omega_p^2}{\omega^2} & 0 \\ 0 & 0 & 1 - \frac{\omega_p^2}{\omega^2} \end{pmatrix} \quad \text{for Plasma} \quad (5)$$

$$\tilde{\epsilon} = \epsilon_0 \begin{pmatrix} 1 & 0 & 0 \\ 0 & 1 & 0 \\ 0 & 0 & 1 - \frac{\omega_{b0}^2/\gamma_0^3}{\omega^2(1 - kV_0/\omega)^2} \end{pmatrix} \quad \text{for Electron Beam} \quad (6)$$

$$\tilde{\epsilon} = \epsilon_0 \begin{pmatrix} \epsilon_r & 0 & 0 \\ 0 & \epsilon_r & 0 \\ 0 & 0 & \epsilon_r \end{pmatrix} \quad \text{for Dielectric} \quad (7)$$

In above equations, $j = \sqrt{-1}$, k and ω are the wave number and frequency, respectively; $\gamma_0 = 1/(1 - V_0^2/c^2)^{1/2}$, plasma frequency is related to plasma density

as $\omega_p^2 = \frac{N_{p0}e^2}{m_0\varepsilon_0}$ and $\omega_{b0}^2 = \frac{N_{b0}e^2}{m_0\varepsilon_0}$. Now, we write explicitly the cartesian components of the main Equations (3) and (4) as follows:

$$\begin{cases} \frac{\partial E_z}{\partial y} - jkE_y - j\omega B_x = 0, \\ jkE_x - \frac{\partial E_z}{\partial x} - j\omega B_y = 0, \\ \frac{\partial E_y}{\partial x} - \frac{\partial E_x}{\partial y} - j\omega B_z = 0, \end{cases} \quad (8)$$

$$\begin{cases} \frac{\partial B_z}{\partial y} - jkB_y + j\frac{\omega}{c^2}\epsilon_x E_x = 0, \\ jkB_x - \frac{\partial B_z}{\partial x} + j\frac{\omega}{c^2}\epsilon_y E_y = 0, \\ \frac{\partial B_y}{\partial x} - \frac{\partial B_x}{\partial y} + j\frac{\omega}{c^2}\epsilon_z E_z = 0. \end{cases} \quad (9)$$

where in our problem the general form of the dielectric tensor $\tilde{\varepsilon}$ is as follows:

$$\tilde{\varepsilon} = \varepsilon_0 \begin{pmatrix} \epsilon_x & 0 & 0 \\ 0 & \epsilon_y & 0 \\ 0 & 0 & \epsilon_z \end{pmatrix},$$

for plasma, RPEB and dielectric regions. By solving Equations (8) and (9), we obtain E_x, E_y, B_x and B_y in terms of derivatives of E_z and B_z . Then with considering all of regions together as a whole system, one can write

$$\begin{aligned} \frac{\omega}{c^2} \left[\frac{\partial}{\partial x} \left(\frac{\epsilon_t}{k_t^2} \frac{\partial}{\partial x} \right) + \frac{\partial}{\partial y} \left(\frac{\epsilon_t}{k_t^2} \frac{\partial}{\partial y} \right) \right] E_z + \frac{k}{c} \left[\frac{\partial}{\partial x} \left(\frac{1}{k_t^2} \frac{\partial}{\partial y} \right) - \frac{\partial}{\partial y} \left(\frac{1}{k_t^2} \frac{\partial}{\partial x} \right) \right] cB_z \\ = \frac{\omega}{c^2} \epsilon_z E_z, \end{aligned} \quad (10)$$

$$\begin{aligned} k \left[\frac{\partial}{\partial y} \left(\frac{1}{k_t^2} \frac{\partial}{\partial x} \right) - \frac{\partial}{\partial x} \left(\frac{1}{k_t^2} \frac{\partial}{\partial y} \right) \right] E_z + \frac{\omega}{c} \left[\frac{\partial}{\partial x} \left(\frac{1}{k_t^2} \frac{\partial}{\partial x} \right) + \frac{\partial}{\partial y} \left(\frac{1}{k_t^2} \frac{\partial}{\partial y} \right) \right] cB_z \\ = \frac{\omega}{c} cB_z, \end{aligned} \quad (11)$$

where $\epsilon_t = \epsilon_x = \epsilon_y$ for each region can be defined according to Equations (5)-(7) and $k_t^2 = \epsilon_t \frac{\omega^2}{c^2} - k^2$. As already explained in Ref. [13], for a propagation along the z -axis, in an elliptical structure with several boundaries only hybrid waves are permitted to be excited and propagated. Therefore, generally in the elliptical waveguides, the waves are hybrid and only for the special problem including an absolutely homogeneous elliptical waveguide, waves can be divided into two independent TE and TM modes. Now, after obtaining the governing equations of longitudinal electric and magnetic fields, we are going to investigate the dispersion diagram and the growth rate of excited waves in the waveguide. In the following section, making use of FEM and meshing the structure, we will consider the impact of different parameters on the growth rate, numerically.

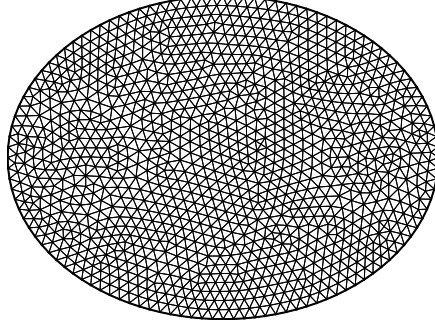


Figure 2: Meshing of geometric schematic of under study waveguide performed by the FEM.

3. Dispersion Equation and Time Growth Rate by Numerical Simulation

In this part, the region of under study waveguide region is divided to a number $O(10^5)$ triangular finite elements. The triangular elements are indexed by $e = 1, \dots, N$, where N is the whole number of elements. An example of meshing of the novel elliptical waveguide is plotted in Figure 2. The electric and magnetic fields in e 'th element are defined as follow:

$$E_z^{(e)}(x, y) = \sum_{i=1}^3 \Phi_i^{(e)}(x, y) \Psi_i$$

$$cB_z^{(e)}(x, y) = \sum_{i=1}^3 \Phi_i^{(e)}(x, y) \Psi_i' . \quad (12)$$

where $\Phi_i^{(e)}(x, y)$ are the interpolation functions and Ψ_i and Ψ_i' are the unknown numerical values of the E_z and cB_z at the nodes, respectively. By using Equations (10) and (11), the action integral F is introduced in following form:

$$F = \frac{1}{2} \frac{\omega}{c^2} \int d\Omega \left\{ \frac{\epsilon_t}{k_t^2} \left(\left(\frac{\partial E_z}{\partial x} \right)^2 + \left(\frac{\partial E_z}{\partial y} \right)^2 \right) + \frac{1}{k_t^2} \left(\left(\frac{\partial cB_z}{\partial x} \right)^2 + \left(\frac{\partial cB_z}{\partial y} \right)^2 \right) \right\} \quad (13)$$

$$+ \frac{2\delta}{k_t^2} \left(\frac{\partial E_z}{\partial x} \frac{\partial cB_z}{\partial y} - \frac{\partial E_z}{\partial y} \frac{\partial cB_z}{\partial x} \right) - \epsilon_z E_z^2 - (cB_z)^2 \Big\},$$

where $\delta = kc/\omega$, $d\Omega = dx dy$. The action integral F must be optimized [6]. With substituting Equations (12) in action integral F , Equation (13), the equations of optimization are:

$$\frac{\partial F}{\partial \Psi_i} = 0, \quad \frac{\partial F}{\partial \Psi'_i} = 0$$

The matrix form of above equations can be written as:

$$\begin{bmatrix} A_{ij} & C_{ij} \\ \tilde{C}_{ij} & A'_{ij} \end{bmatrix} \vec{\Psi}^{(e)} = k^2 \begin{bmatrix} B_{ij} & 0 \\ 0 & B'_{ij} \end{bmatrix} \vec{\Psi}^{(e)}, \quad (14)$$

where

$$A_{ij} = (\epsilon_i - \beta_i \frac{\omega_p^2}{\omega^2}) A^+ + \left((\epsilon_i - \beta_i \frac{\omega_p^2}{\omega^2} - \delta^2) \frac{\omega_i^2}{\alpha_i^2 c^2} + (\beta_i \omega_p^2 - \epsilon_i \omega^2) \frac{\epsilon_i}{c^2} \right) A^0$$

$$A'_{ij} = A^+ + \left(\beta_i \frac{\omega_p^2}{c^2} - \epsilon_i \frac{\omega^2}{c^2} \right) A^0$$

$$C_{ij} = 2\delta A^-, B_{ij} = \epsilon_i A^0, B'_{ij} = A^0,$$

and the matrices A_{ij}^α with $\alpha = +, -, 0$ are the two-dimensional spatial integrals of derivatives of the interpolation functions $\Phi_i^{(e)}(x, y)$ with respect to x and y [28]. Here, $\vec{\Psi}^{(e)}$ is the elemental unknown vector including six components Ψ_i and Ψ'_i . After the augmentation processes on the elemental matrices and vectors in Equations (14), the global generalized eigenvalue equation $A \vec{\Psi} = k^2 / \delta^2 A^0 \vec{\Psi}$ is obtained which can be solved by the LAPACK routines.

In this section, in addition the dispersion diagram, the growth rate of slow waves are studied. By comparing the growth rate of different configurations, the optimal configuration for amplifying waves in this waveguide is selected. Afterwards, the effects of dielectric permittivity and current density of electron beam on the growth rate of the selected configuration will be examined. In the present waveguide, we have chosen semi-interfocal distance and the normalized plasma frequency as $\omega_p a/c = 2.5$, $f = 1.32 cm$, where a is semi-major axis of the waveguide. It should be noted that in all of the examined situations, the center of the plasma column is exactly on left focus of the elliptic waveguide. In configuration I, the radius of plasma and electron beam columns are $R_p = f/3$ and $R_b = f/4$, respectively, and the beam center has been placed in right focus of the waveguide that means $\theta_b = 0$. The frequency spectra for hybrid modes excited in configuration I is presented in Figure 3. As known, the energy sources can be a generator for instability of the systems. In the presented waveguide, the electron beam as an

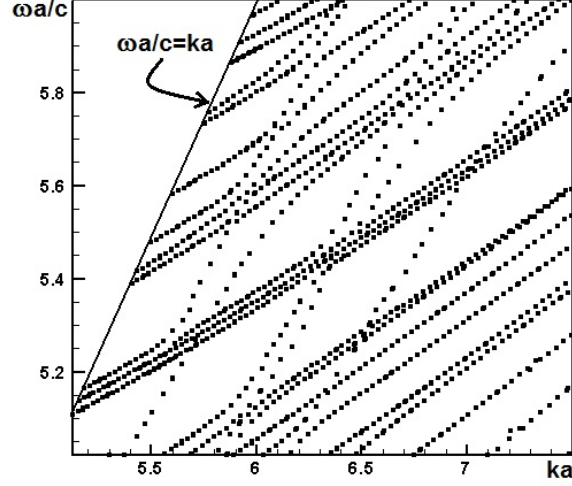


Figure 3: Dispersion characteristic of slow waves in the elliptical plasma waveguide involving an isotropic cold plasma circular column in the presence of the RPEB. Input parameters are: $\epsilon_r = 4.2$, $i_b = 10A$, $\Delta\Phi = 100kV$ and $R_p = f/3$, $R_b = f/4$, $\theta_b = 0$.

energy source can amplify the slow waves with phase velocity less than c , $\omega/k < c$. In this frequency range velocity of the beam particles can be faster than the phase velocity of the wave. While overtaking the wave, the electrons will be slowed down by the electric field of the wave. Thus kinetic energy from the beam particles is transformed to the slow wave and owing to the well-known phenomenon of Cherenkov radiation, the wave amplitude grows. The growth rate of slow wave excited in the waveguide with configuration I is shown in Figure 4.

In configuration II, the radius of plasma and electron beam columns are $R_p = f/3$ and $R_b = f/5$, respectively and $\theta_b = 0$. The normalized growth rate for configuration II is plotted in Figure 5. In third configuration, the plasma radii is decreased to $R_p = f/4$ and its effect on normalized growth rate is seen in Figure 6. Comparison between the normalized growth rates, Ga/c , in configurations I-III of the novel waveguide shows by reducing of electron beam radius, the growth rate increases. More focusing of the RPEB results greater synergy of the electrons energy and therefore the wave amplification enhances. On the other hand by decreasing plasma radius, growth rate decreases. This happens since active region of the waveguide i.e. plasma gets smaller and efficient longitudinal electric field will be reflected less into it. In the following, by shifting electron beam from the waveguide focus, the effect of the beam location on amplifying of slow waves is studied in configurations IV and V. Growth rate diagram of configurations IV with parameters $R_p = f/3$, $R_b = f/5$ and $\theta_b = \pi/16rad$ is presented in Figure 7. In

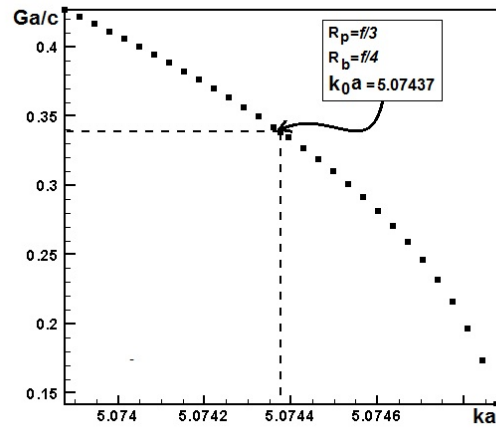


Figure 4: The normalized growth rate for configuration I of the novel elliptical plasma waveguide. Input parameters are similar to Figure 3 and associated operating frequency is $\omega_0 a/c = 4.57080$.

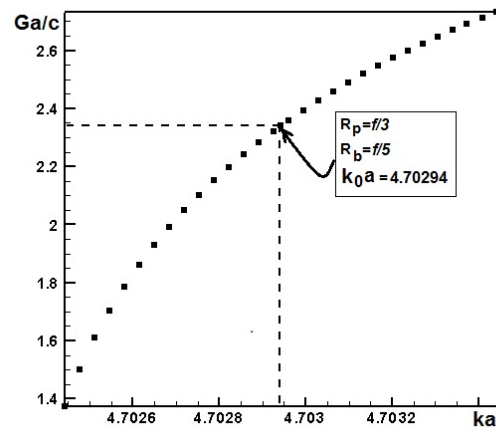


Figure 5: The normalized growth rate for configuration II of the novel elliptical plasma waveguide. Here $R_b = f/5$ and the other parameters are similar to Figure 3. The associated operating frequency is $\omega_0 a/c = 4.08185$.

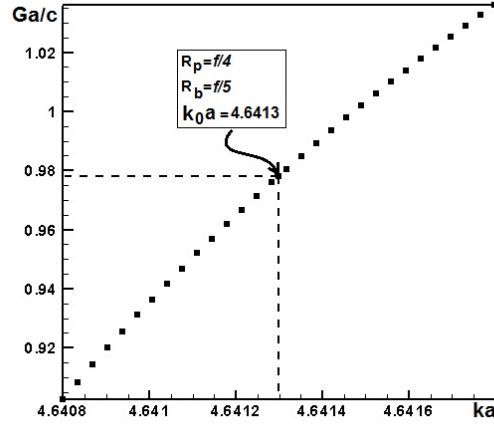


Figure 6: The normalized growth rate for configuration III of the novel elliptical plasma waveguide. Here $R_p = f/4$ and other input parameters are similar to Figure 5 and associated operating frequency is $\omega_0 a/c = 4.06517$.

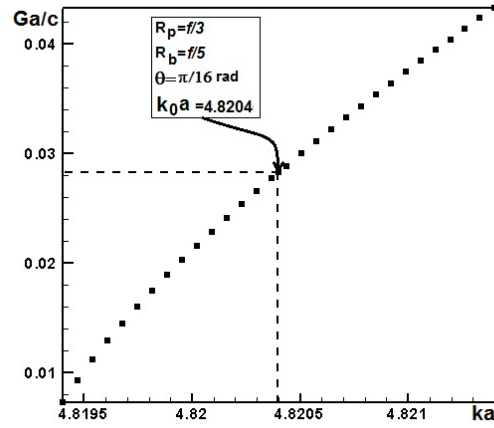


Figure 7: The normalized growth rate for configuration IV of the novel elliptical plasma waveguide. Here $\theta_b = \pi/16 \text{ rad}$ and other input parameters are similar to Figure 5. Associated operating frequency is $\omega_0 a/c = 3.87881$.

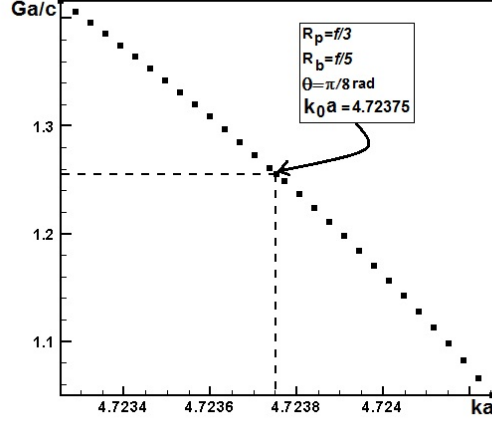


Figure 8: The normalized growth rate for configuration V of the novel elliptical plasma waveguide. Here $\theta_b = \pi/8rad$ and other input parameters are similar to Figure 5. Associated operating frequency is $\omega_0 a/c = 3.97951$.

configurations V displacement of beam from focus is increased to $\theta_b = \pi/8rad$ and the result has been shown in Figure 8.

The outcome derived from Figures 5,7 and 8 is that the optimal structure of the present waveguide to amplify the slow wave will be found when the electron beam is located on the focus. In this situation, the maximum energy transfers from the energy source, namely, RPEB to the electromagnetic active medium of the waveguide, namely the plasma column. In addition, the impact of relative permittivity of dielectric ϵ_r , and the beam current on growth rate in a fixed structure of the novel waveguide (configuration II), have been investigated. Diagram plotted in Figure 9 in comparing with Figure 5 indicates that with increasing the permittivity of dielectric from $\epsilon_r = 4.2$ to $\epsilon_r = 6$, the the growth rate increases. Figure 10 shows the variation of normalized growth rate Ga/c versus normalized wavelength ka for three distinctive beam currents, (a) $i_b = 50A$, (b) $500A$ and (c) $1kA$, respectively. As seen from these figures, with increasing the beam current, the normalized growth rate increases.

By considering above growth rate diagrams, it can be obtained the optimum design of under study elliptical waveguide with the criterion of maximum growth rate. In this slow-wave plasma-dielectric waveguide, Cherenkov instability phenomenon is the cause of wave radiation. Spontaneous Cherenkov radiation will occur when the electron velocity is comparable or higher than the phase velocity of electromagnetic waves [1]. By increasing the current intensity of RPEB, plasma frequency of beam or number of relativistic electrons increases that leads to more

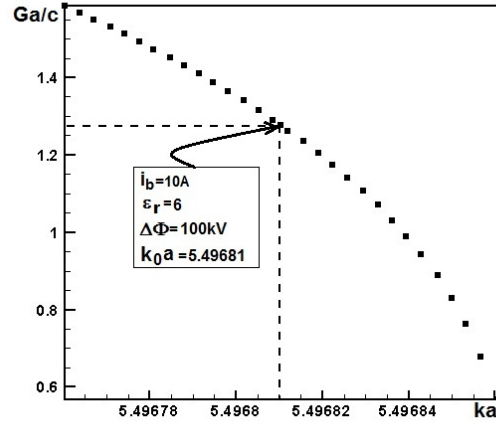


Figure 9: The impact of dielectric permittivity on the growth rate. Here $\epsilon_r = 6$ and related operating frequency $\omega_0 a/c = 4.01429$. The further parameters are similar to Figure 3.

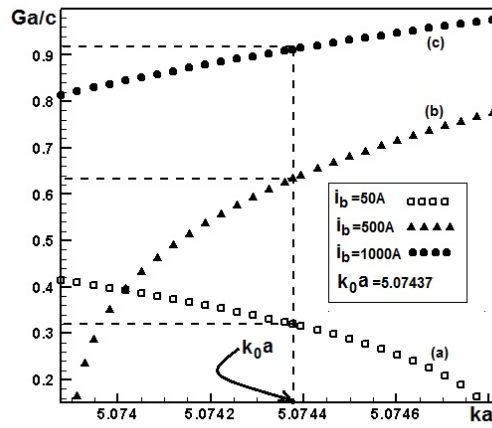


Figure 10: The impact of electron beam current i_b on the growth rate for a fixed operating frequency $\omega_0 a/c = 4.57080$. Here (a) $i_b = 50A$, (b) $i_b = 500A$, (c) $i_b = 1kA$ and the further parameters are similar to Figure 3.

energy transfer to the wave and amplification of the slow wave rises.

Also, by following the figures one can find that in a configuration with the minor beam radius and the major plasma radius, growth rate of the slow waves in the waveguide will enhance. This result is due to the fact that RPEB as a energy source in the medium, causes that slow waves are driven to instability and amplification. Also plasma column is an energetic electromagnetic region in which the electron beam can interplay with the longitudinal electric field of wave [15]. Therefore increasing of the active area and the more concentration of energetic electrons of RPEB in the waveguide focus, will increase interaction between the particle and wave and as a result energy transportation to the slow waves will be increased.

4. Summary and Conclusion

In this research, the excitation and amplification of slow waves in an elliptical dielectric waveguide including relativistic electron beam and isotropic plasma columns, were studied. We supposed relativistic pencil electron beam has been focused by an intense external magnetic field so that transverse motion of electrons in the beam were trivial small. The allowed mode spectrum in the presence of RPEB had been numerically calculated by finite element method. In addition, growth rate of the excited waves owing to interaction with the electron beam was computed. The influences of different geometric configurations that were marked by configurations I-V, the electron current, and dielectric permittivity on the growth rate have been investigated. By scrutinizing the growth rate, this result was obtained that wave amplification increases by dwindling the radius of RPEB. It was found the more growth rates would be obtained for larger radius of plasma column, as well. Moreover, the investigation of effect of the dielectric permittivity showed that with increasing dielectric constant, the normalized growth rate increased. On the other hand, we demonstrated by increasing the current intensity, the growth rate increases in a fixed voltage. Finally, it was concluded that the optimal design to achieve the maximum wave amplification is related to the configuration *II* including the RPEB with a current of $i_b = 1kA$, and dielectric constant equal with $\epsilon_r = 6$ for dielectric material inside the waveguide.

Conflicts of Interest. The author declares that there are no conflicts of interest regarding the publication of this article.

References

- [1] A. F. Alexandrov, L. S. Bogdankovich and A. A. Rukhadze, *Principle of Plasma Electrodynamics*, Springer, Heidelberg, 1984.

-
- [2] A. C. Boucouvalas, C. Papageorgiou and E. Georgantzios, Elliptical fibre dielectric waveguides: a transverse transmission line analysis, *IET Optoelectronic* **14** (2020) 1 – 9.
- [3] C. Bowness, On the Efficiency of Single and Multiple Elliptical Laser Cavities, *Appl. Opt.* **4** (1965) 103 – 107.
- [4] B. Gimeno and M. Guglielmi, Full wave network representation for rectangular, circular, and elliptical to elliptical waveguide junctions, *IEEE Trans. Microw. Theory Tech.* **45** (1997) 376 – 384.
- [5] B. Jazi, Z. Rahmani, E. Heidari-Semiromi and A. Abdoli-Arani, Time growth rate and field profiles of hybrid modes excited by a relativistic elliptical electron beam in an elliptical metallic waveguide with dielectric rod, *Phys. Plasmas* **19** (2012) 102110.
- [6] J. Jin, *The Finite Element Method in Electromagnetics* John Wiley and Sons. Inc, New York, 2002.
- [7] V. Kamra and A. Dreher, Analysis of elliptical waveguides with anisotropic dielectric layers, *IEEE Access* **8** (2020) 31444 – 31452.
- [8] M. Lu, Z. Hu, Z. Peng, X. Chen, F. Xu, K. Zhao, M. Matsumoto, F. Wei and Zh. Yang, Finite element analysis of the dominant mode variation in groove guide, *Int. J. Infrared Millimeter Waves* **21** (2000) 63 – 76.
- [9] M. Lu and P. Leonard, Edge based finite element analysis of the field patterns in V-shaped microshield line, *Microw. Opt. Technol. Lett.* **41** (2004) 43 – 47.
- [10] N. Marcuritz (Ed.), *Waveguide Handbook*, Mc Graw-Hill, New York, 1951.
- [11] K. Okamoto, *Fundamentals of Optical Waveguides*, Academic press, New York, 2000.
- [12] S. J. Orfanidis, *Electromagnetic Waves and Antennas*, ECE Department, Rutgers University, 2016.
- [13] Z. Rahmani, E. Heidari-Semiromi, A. Abdoli-Arani, Study on the influence of two relativistic circular electron beam columns placed in an elliptical dielectric waveguide on excitation and amplification of electromagnetic waves using finite-element method, *IEEE Trans. Plasma Sci.* **47** (2019) 1254 – 1261.
- [14] Z. Rahmani, E. Heidari-Semiromi and S. Safari, Excitation of THz hybrid modes in an elliptical dielectric rod waveguide with a cold collisionless unmagnetized plasma column by an annular electron beam, *Phys. Plasmas* **23** (2016) 062113.

- [15] Z. Rahmani, B. Jazi and E. Heidari-Semiromi, Terahertz electromagnetic wave generation and amplification by an electron beam in the elliptical plasma waveguides with dielectric rod, *Phys. Plasmas* **21** (2014) 092122.
- [16] S. M. Saad, Review of numerical methods for the analysis of arbitrarily-shaped microwave and optical dielectric waveguides, *IEEE Trans. Microw. Theory Tech.* **33** (1985) 894 – 899.
- [17] S. P. Savaidis and J. A. Roumeliotis, Scattering by an infinite circular dielectric cylinder coating eccentrically an elliptic dielectric cylinder, *IEEE Trans. Antennas Propag.* **52** (2004) 1180 – 1185.
- [18] S. P. Savaidis and J. A. Roumeliotis, Scattering by an infinite elliptic dielectric cylinder coating eccentrically a circular metallic or dielectric cylinder, *IEEE Trans. Microw. Theory Tech.* **45** (1997) 1792 – 1800.
- [19] A. K. Shahi, V. Singh and S. P. Ojha, Dispersion characteristics of electromagnetic waves in circularly cored highly birefringent waveguide having elliptical cladding, *Prog. Electromagn Res. Pier.* **75** (2007) 51 – 62.
- [20] Y. Shen and V. Giurgiutiu, Combined analytical FEM approach for efficient simulation of Lamb wave damage detection, *Ultrasonics* **69** (2016) 116-128.
- [21] S. Shiraiwa, O. Meneghini, R. Parker, P. Bonoli, M. Garrett, M. C. Kaufman, J. C. Wright and S. Wukitch, Plasma wave simulation based on a versatile finite element method solver, *Phys. Plasmas* **17** (2010) 056119.
- [22] C. Vassallo, *Optical Waveguide Concepts*, Elsevier, Amsterdam, Chap. 3-3, 1991.
- [23] G. P. Zouros and J. A. Roumeliotis, Scattering by an Infinite Dielectric Cylinder Having an Elliptic Metal Core: Asymptotic Solutions, *IEEE Trans. Antennas. Propag.* **58** (2010) 3299 – 3309.

Zeinab Rahmani
Department of Laser and Photonics,
Faculty of Physics,
University of Kashan, Kashan,
Islamic Republic of Iran
e-mail: z.rahmani@kashanu.ac.ir